

RESEARCH LETTER

10.1002/2015GL066612

Key Points:

- Melt rates greater than 20 m/yr occur locally beneath the Ross Ice Shelf
- Channels can be created by highly concentrated melting in the grounding zone
- Relict channels may be indicators of subglacial discharge reorganization

Supporting Information:

- Supporting Information S1
- Figure S1

Correspondence to:

O. J. Marsh,
oliver.marsh@canterbury.ac.nz

Citation:

Marsh, O. J., H. A. Fricker, M. R. Siegfried, K. Christianson, K. W. Nicholls, H. F. J. Corr, and G. Catania (2016), High basal melting forming a channel at the grounding line of Ross Ice Shelf, Antarctica, *Geophys. Res. Lett.*, 43, doi:10.1002/2015GL066612.

Received 15 OCT 2015

Accepted 1 DEC 2015

High basal melting forming a channel at the grounding line of Ross Ice Shelf, Antarctica

Oliver J. Marsh^{1,2}, Helen A. Fricker¹, Matthew R. Siegfried¹, Knut Christianson³, Keith W. Nicholls⁴, Hugh F. J. Corr⁴, and Ginny Catania⁵

¹Institute for Geophysics and Planetary Physics, Scripps Institution of Oceanography, University of California, San Diego, La Jolla, California, USA, ²Gateway Antarctica, University of Canterbury, Christchurch, New Zealand, ³Department of Earth and Space Science, University of Washington, Seattle, Washington, USA, ⁴British Antarctic Survey, Cambridge, UK, ⁵Institute for Geophysics, University of Texas at Austin, Austin, Texas, USA

Abstract Antarctica's ice shelves are thinning at an increasing rate, affecting their buttressing ability. Channels in the ice shelf base unevenly distribute melting, and their evolution provides insight into changing subglacial and oceanic conditions. Here we used phase-sensitive radar measurements to estimate basal melt rates in a channel beneath the currently stable Ross Ice Shelf. Melt rates of $22.2 \pm 0.2 \text{ m a}^{-1}$ (>2500% the overall background rate) were observed 1.7 km seaward of Mercer/Whillans Ice Stream grounding line, close to where subglacial water discharge is expected. Laser altimetry shows a corresponding, steadily deepening surface channel. Two relict channels to the north suggest recent subglacial drainage reorganization beneath Whillans Ice Stream approximately coincident with the shutdown of Kamb Ice Stream. This rapid channel formation implies that shifts in subglacial hydrology may impact ice shelf stability.

1. Introduction

Floating ice shelves around Antarctica are thinning substantially, driven primarily by melting at the ice-ocean interface [Paolo *et al.*, 2015; Rignot *et al.*, 2013]. On a regional scale this thinning is well mapped, but small-scale local melt patterns are not well known. Uneven melt distribution leading to channel formation may significantly influence the total mass loss of ice shelves and alter their buttressing ability, surface velocity, and basal melt rates [Stanton *et al.*, 2013; Drews, 2015; Millgate *et al.*, 2013]. Surface expressions of these ice shelf basal channels are widespread and observed in satellite imagery [Le Brocq *et al.*, 2013; Langley *et al.*, 2014]. Mechanisms proposed for channel formation include the following: thinning and softening of the ice due to lateral shearing at ice shelf margins [Sergienko, 2013], local deformation by basal topography as the ice moves across the grounding line [Gladish *et al.*, 2012], and melting from buoyancy-driven meltwater plumes initiated by freshwater input from beneath grounded ice [Jenkins, 2011]. While these mechanisms are not mutually exclusive, physical processes occurring at the ice-ocean interface are poorly understood, particularly near the grounding line. There are few direct observations of basal melt rates in channels [Stanton *et al.*, 2013; Dutrieux *et al.*, 2014], and the little information we have about channel formation and evolution comes from sparse radar and satellite data. Hence, channels may either protect ice shelves from excessive melt [Gladish *et al.*, 2012; Millgate *et al.*, 2013] or contribute to their structural weakening [Vaughan *et al.*, 2012; Rignot and Steffen, 2008], and the net effect of basal channels on ice shelf stability is uncertain.

In this paper we present the first direct estimates of basal melt rates from a major subglacial channel in the southern Ross Ice Shelf (RIS), using phase-sensitive radar data (Figure 1). The subglacial channel we surveyed is located at the suture zone of the Mercer and Whillans Ice Streams, which feed RIS from West Antarctica. This region of RIS has spatially averaged basal melt rates of less than 0.5 m a^{-1} [Moholdt *et al.*, 2014]. We created a new grounding-zone flexure map using TerraSAR-X interferometry from 2012 and mapped the surface extent of the channel in Moderate Resolution Imaging Spectroradiometer (MODIS) imagery (Text S1 in the supporting information). Ice flow is parallel to the grounding line, and the channel is aligned with flow within the tidal flexure zone with a visible surface expression extending 55 km onto the ice shelf. Comparison of MODIS data from 2004, 2009, and 2014 shows that the channel develops in the upper few kilometers and all channel features advect downstream with ice flow (Figure S1). Ice-penetrating radar data from 2006 confirm a basal channel of similar width, with amplitude of up to 60–80 m at the downstream end (Figure S2).

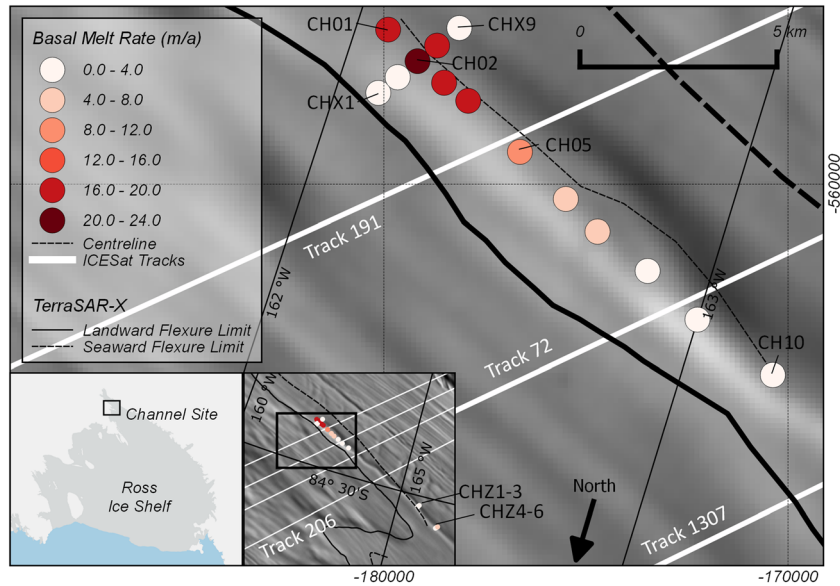


Figure 1. Basal melt rates in and around an ice shelf basal channel at the grounding zone of Mercer Ice Stream, with landward (black solid) and seaward (black dashed) limits of flexure from TerraSAR-X in 2012. Background image is MODIS Mosaic of Antarctica (MOA; S1). Inset: Full extent of the main channel and location of additional radar data and ICESat tracks referred to in the supporting information.

2. Local Melt Rate Measurements

We occupied 25 points in and around the channel with a phase-sensitive radar system over a 38 day period from December 2014 to January 2015 (Table S1). Phase-sensitive radar allows precise measurements of ice thickness and vertical strain between internal layers in the ice column, and repeat measurements can be differenced to derive ice thinning rates [Corr *et al.*, 2002; Brennan *et al.*, 2014]. We estimated thinning of between 15 and 22 m a^{-1} at five sites (CH01–CH05) at the upstream end of the channel (Figure 1). This thinning is confined to the center of the channel and composed of less than 1% strain thinning (around $1 \times 10^{-4} \text{ a}^{-1}$); we attribute the remainder to basal melting. The melt rate decreases with distance downstream along the channel centerline to $11.8 \pm 0.3 \text{ m a}^{-1}$ after 3 km (CH05), $3.9 \pm 0.2 \text{ m a}^{-1}$ after 10 km (CH10), and $2.5 \pm 0.2 \text{ m a}^{-1}$ after 40 km (CHZ3). On the ice shelf 1 km across flow from the channel centerline we estimate a melt rate of $0.82 \pm 0.07 \text{ m a}^{-1}$ (CHX9), indicative of the background ice shelf melt rate. We calculated errors at each location using the RMS from a linear fit to all data points (Text S7). Measurements repeated approximately weekly in the channel show small variability in thinning over the acquisition period (Figure S3) and no correlation with ocean tidal amplitude.

We extended our observation period by monitoring channel evolution at the surface using satellite data. Surface elevation does not exactly mirror basal topography over the channel; this is expected as the ice shelf is not in full hydrostatic equilibrium within the grounding zone. Nevertheless, temporal changes in surface elevation provide a broad indication of changes at the base. At the surface, the channel is between 1 and 2 km wide and up to 10 m deeper than the adjacent ice shelf; the width decreases and the channel becomes shallower downstream. Ice, Cloud and land Elevation Satellite (ICESat) laser altimetry indicates that along most of its length, the depth of the surface depression remained constant between 2003 and 2009 (Track 206) but that it deepened and slightly widened at the upstream end (Tracks 191, 72, and 1307; Figure 2). Its cross-sectional area at the upstream end increased at a constant rate by $1400 \text{ m}^2 \text{ a}^{-1}$ over this period. Consistent surface lowering of 0.5 m a^{-1} averaged across the full width of the upper channel (Figure 2) implies a melt rate of $\sim 5 \text{ m a}^{-1}$ in an Eulerian (not moving) reference frame, when combined with extensional horizontal strain data in a mass conservation approach (Texts S3–S5). This satellite-inferred melt rate is lower than the phase-sensitive radar measurements, but the narrowly focused melting we observed using phase-sensitive radar at the channel base is likely to be distributed over a wider area in the surface response [Vaughan *et al.*, 2012].

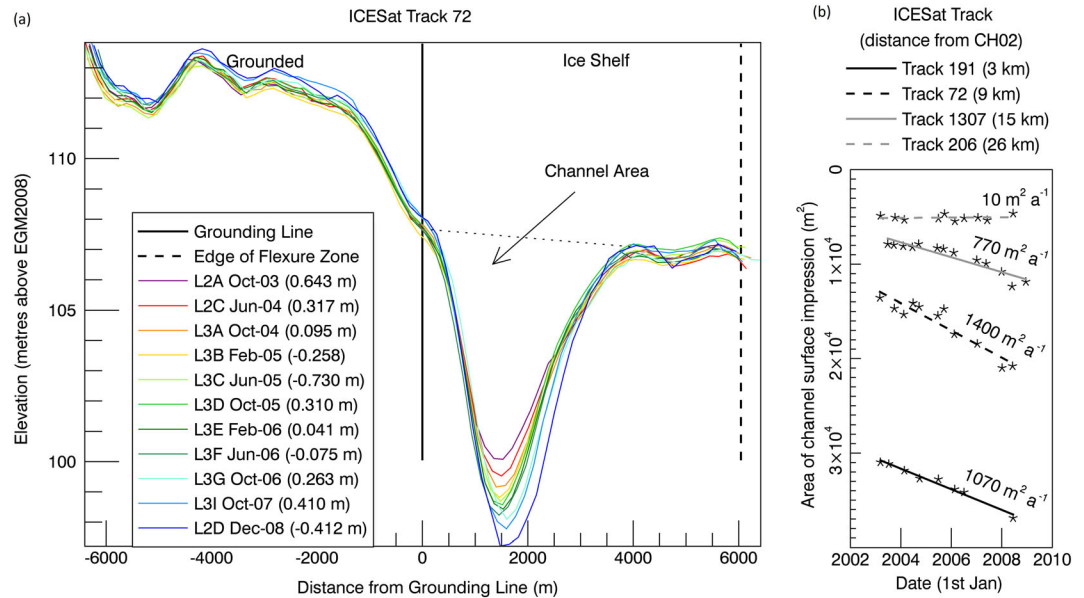


Figure 2. Change in surface expression of the channel over the ICESat period (2003–2009). (a) ICESat surface elevation profiles along Track 72, perpendicular to the channel and grounding line at the upstream end (see Figure 1 for location). (b) Channel growth estimated from four ICESat tracks that cross the basal channel; distance from the location of highest melting (CH02) is given. Elevations are corrected for ocean tides using a regional tide model (CATS2008a_opt; tides from freely floating ice shelf at 84.635°S, 163.5°W in parentheses). The correction accounts for location within the flexure zone (zero correction on grounded ice, full correction on fully floating ice).

Our local melt rates of 15 to 22 m a⁻¹ are an order of magnitude higher than regional average values predicted by ocean models of the Ross Ice Shelf cavity [Dinniman *et al.*, 2007], inferred from remote sensing analysis [Moholdt *et al.*, 2014] and estimated from radar data at the Kamb Ice Stream grounding line farther north [Catania *et al.*, 2010]. Although melting can be enhanced in grounding zones [Rignot and Jacobs, 2002], such high rates are unlikely to be solely due to tidal mixing [Makinson *et al.*, 2011], as tidal currents in this region are low. Ocean temperatures in this part of the Ross Ice Shelf are likely to be below -1.5°C [MacAyeal, 1984], although sinuous grounding-zone geometry means that this embayment may not be representative of the wider area. Our estimated melt rates are highest where the basal channel is not yet fully established and cannot be solely a result of the focusing effect of ice shelf basal topography on ocean currents [Stanton *et al.*, 2013]. The most likely cause for this locally enhanced melting is subglacial freshwater discharge [Jenkins, 2011].

3. Subglacial Hydrology

Active subglacial lakes exist across Whillans Ice Plain [Fricker and Scambos, 2009], and the subglacial hydrological system in this area drains meltwater from a large region of West Antarctica including the upper Whillans and Kamb basins [Carter and Fricker, 2012]. The main outflow for subglacial meltwater was predicted from a local hydropotential map to occur approximately 50 km farther to the south than the channel initiation zone [Carter and Fricker, 2012] (Figure 3); however, Whillans Ice Plain has an exceptionally flat hydropotential surface, and major switches in drainage pathways can be caused by only moderate changes (~2 m) in ice thickness [Carter *et al.*, 2013]. A change of this magnitude is entirely possible given the uncertainty in basal topography and what is known about thickness fluctuations in these ice streams. Kamb Ice Stream stagnated around 150 years ago [Catania *et al.*, 2012], and Whillans Ice Stream is currently slowing by 1–2% per year, toward a possible stagnation early next century [Beem *et al.*, 2014]. In response to these dynamical changes, Kamb has thickened and the southern Whillans Ice Plain and Mercer Ice Stream have experienced overall thinning over the last 60 years [Winberry *et al.*, 2014]. Thinning of the Whillans and Mercer Ice Streams and thickening of the Kamb resulting in less than ~20 m overall change in relative surface elevation between these systems would provide sufficient change in hydropotential to divert the main

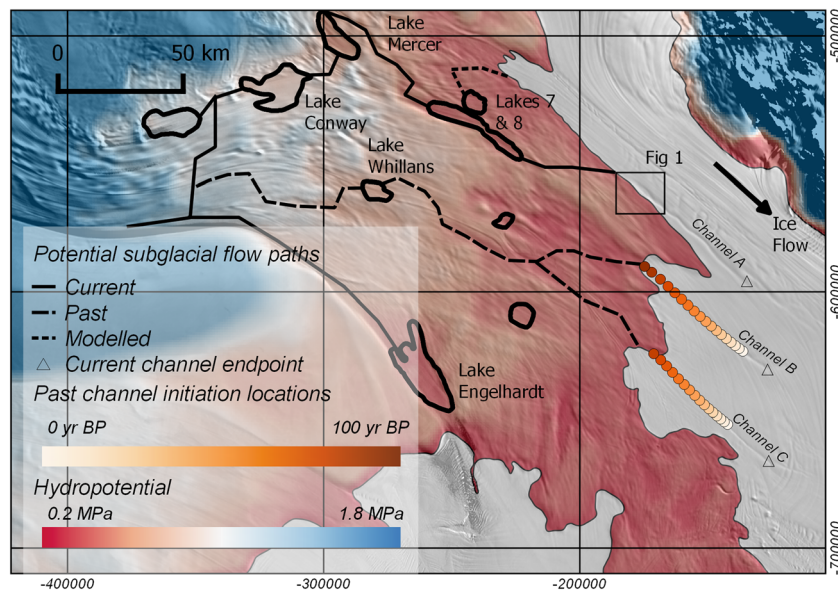


Figure 3. Subglacial hydrologic system of the Whillans Ice Plain. Colored field shows the hydropotential map (Text S8) with active subglacial lakes outlined in black. The current, past, and previously modeled flow paths are shown. Orange circles correspond to the approximate past location of the initiation point of Channels B and C, based on extrapolation of interferometric synthetic aperture radar velocity difference between 1997 and 2009 [Scheuchl *et al.*, 2012]. Background image is MOA [Scambos *et al.*, 2007].

outflow of subglacial water from the upper Whillans and Kamb catchments toward the suspected current outlet near Lake 7 (Figure 3).

Lakes Conway, Mercer, 7, and 8 are the closest lakes to the channel initiation zone (Figure 3) and are hydrologically connected, draining episodically for periods of up to a year [Fricker and Scambos, 2009; Siegfried *et al.*, 2014]. Recent GPS data over these lakes show a drainage event during 2013 and the early part of 2014 [Siegfried, 2015]. Using a “reduced model” for convection-driven melting [Jenkins, 2011], we estimate a potential grounding line melt rate of 24 m a^{-1} using an outflow of $\sim 48 \text{ m}^3 \text{ s}^{-1}$ associated with lake drainage [Siegfried *et al.*, 2014]. While there are significant uncertainties in the rate and distribution of subglacial discharge due to sparse oceanographic data and no information about the geometry of the outflow channel (Text S6), a subglacial meltwater plume associated with this lake drainage event is a feasible explanation for such high local melt rates at the grounding line. High basal melt rates during summer 2014–2015 may indicate a period of increased subglacial outflow across the grounding line associated with the preceding lake drainage event, although the hydrological conductivity through the system, and hence timing of discharge across the grounding line, is unclear. As we see neither variable melt rates over our short time series nor any evidence of changes in channel amplitude downstream indicating melt rate variability, further measurements are needed to confirm whether there was particularly high discharge at this time triggered by subglacial lake drainage.

4. Relict Channels as Evidence of Subglacial Hydrology Migration

MODIS imagery reveals surface depressions on the ice shelf to the north of the main channel (Channel A) beginning around 50 km downstream of the 2012 grounding line (Channels B and C; Figure 3). They are not aligned with flow stripes and are similar in surface form and width to Channel A, which suggests they were also formed by strong localized melting. It is unlikely that these channels resulted from shear-induced weakening given that shear stresses are low [Winberry *et al.*, 2014] or from fracturing due to tidal flexure as the tidal amplitude is less than 1 m. ICESat-derived estimates of surface elevation change suggest that none of the channels are currently deepening outside the immediate grounding-zone area. We propose that Channels B and C originally formed during periods of high localized melting at the ice shelf base caused by meltwater outflow at a stable grounding line and that Channel A continues to expand at its upstream end by the same mechanism.

We can estimate the ages of these surface channels from their lengths and the current ice flow velocity. Extrapolating the regional velocity difference from 1997 to 2009 (a slowdown to approximately 300 m a^{-1})

[Scheuchl *et al.*, 2012] backward in time (Figure 3), we estimate that both these features would have stopped forming at the present-day grounding line between 85 and 120 years ago and were centered in two distinct grounding line embayments at that time. The current length of Channel A (~55 km) suggests that it may have started forming when formation of the other channels ceased—for comparison Channel B is now 52 km from the grounding line. Satellite data from the last 20 to 40 years show recent grounding line stability in this area [Horgan and Anandakrishnan, 2006], but grounding-zone migration and highly variable surface velocities cannot be ruled out given the unstable past ice dynamics. Despite these caveats, the location of relict channels and new ideas about their formation mechanism implies a significantly stronger subglacial outflow to the north between 85 and 120 years ago (or sooner if the grounding line has since retreated), before a switch to the current location. The two relict channels are both relatively short (representing formation times of ~25 years (Channel B) and ~45 years (Channel C) under current velocities), and therefore, any previous subglacial drainage configuration may have been short lived. This is consistent with the changing glacial history of the region [Catania *et al.*, 2012; Beem *et al.*, 2014; Winberry *et al.*, 2014].

5. Conclusions

We have presented direct estimates of high basal melt rates at the grounding line of the southern Ross Ice Shelf. These melt rates occur in the formation zone of a well-defined basal channel and are an order of magnitude higher than beneath the surrounding ice shelf. The region is known to experience large subglacial lake drainage events, and we propose that the channel is formed by enhanced mixing due to a buoyant meltwater plume caused by subglacial outflow from beneath the grounded ice. The variability in melting over short spatial scales (~1 to 2 km), with an order of magnitude higher melt rates one location in the grounding zone, suggests melting due to a freshwater plume and highlights the need for the inclusion of subglacial outflow in ocean models of ice shelf cavities, with finer resolution at the grounding line. The link between basal melting of ice shelves and subglacial discharge is important, as both the focus and strength of this discharge are likely to be a principal control on channel evolution, affecting overall ice shelf mass balance and stability.

Acknowledgments

The authors would like to thank NSF and the WISSARD project (PLR 1439774 and 0838854), NY Air National Guard, UNAVCO, and ASC for logistical support. Esteban Chaves and Sarah Neuhaus provided assistance with data collection in the field. TerraSAR-X data were provided through the HYD2869 project. We thank NASA's ICESat Science Project and the NSIDC for distribution of ICESat data. H.F. would like to thank the John Dove Isaacs Chair funds which supported much of this work. H.F. and M.S. were supported by NASA grant NNX13AP60G. The manuscript was written by O.M. with contributions from all authors. H.F., K.C., O.M., and M.S. conceived the study. O.M., M.S., and G.C. collected, processed, and analyzed phase-sensitive radar, GPS, and ice-penetrating radar data, respectively. O.M. and H.F. processed satellite data. H.C. and K.N. provided radar equipment and assisted O.M. with phase-sensitive radar processing and analysis. Data are available by contacting the authors directly.

References

- Beem, L. H., S. M. Tulaczyk, M. A. King, M. Bougamont, H. A. Fricker, and P. Christoffersen (2014), Variable deceleration of Whillans Ice Stream, West Antarctica, *J. Geophys. Res. Earth Surf.*, *119*, 212–224, doi:10.1002/2013JF002958.
- Brennan, P. V., L. B. Lok, K. Nicholls, and H. Corr (2014), Phase-sensitive FMCW radar system for high-precision Antarctic ice shelf profile monitoring, *IET Radar Sonar Navig.*, *8*(7), 776–786, doi:10.1049/iet-rsn.2013.0053.
- Carter, S. P., and H. A. Fricker (2012), The supply of subglacial meltwater to the grounding line of the Siple Coast, West Antarctica, *Ann. Glaciol.*, *53*(60), 267–280, doi:10.3189/2012AoG60A119.
- Carter, S. P., H. A. Fricker, and M. R. Siegfried (2013), Evidence of rapid subglacial water piracy under Whillans Ice Stream, West Antarctica, *J. Glaciol.*, *59*(218), 1147–1162, doi:10.3189/2013JoG13J085.
- Catania, G., C. Hulbe, and H. Conway (2010), Grounding-line basal melt rates determined using radar-derived internal stratigraphy, *J. Glaciol.*, *56*(197), 545–554, doi:10.3189/002214310792447843.
- Catania, G., C. Hulbe, H. Conway, T. A. Scambos, and C. F. Raymond (2012), Variability in mass flux of the Ross ice streams, West Antarctica over the last millennium, *J. Glaciol.*, *58*(210), 741–752, doi:10.3189/2012JoG11J219.
- Corr, H. F. J., A. Jenkins, K. W. Nicholls, and C. S. M. Doake (2002), Precise measurement of changes in ice-shelf thickness by phase-sensitive radar to determine basal melt rates, *Geophys. Res. Lett.*, *29*(8), 1232, doi:10.1029/2001GL014618.
- Dinniman, M. S., J. M. Klinck, and W. O. Smith (2007), Influence of sea ice cover and icebergs on circulation and water mass formation in a numerical circulation model of the Ross Sea, Antarctica, *J. Geophys. Res.*, *112*, C11013, doi:10.1029/2006JC004036.
- Drews, R. (2015), Evolution of ice-shelf channels in Antarctic ice shelves, *Cryosphere*, *9*, 1169–1181, doi:10.5194/tc-9-1169-2015.
- Dutrieux, P., C. Stewart, A. Jenkins, K. W. Nicholls, H. F. J. Corr, E. Rignot, and K. Steffen (2014), Basal terraces on melting ice shelves, *Geophys. Res. Lett.*, *41*, 5506–5513, doi:10.1002/2014GL060618.
- Fricker, H. A., and T. Scambos (2009), Connected subglacial lake activity on lower Mercer and Whillans Ice Stream, West Antarctica, 2003–2008, *J. Glaciol.*, *55*(190), 303–315, doi:10.3189/002214309788608813.
- Gladish, C. V., D. M. Holland, P. R. Holland, and S. F. Price (2012), Ice-shelf basal channels in a coupled ice/ocean model, *J. Glaciol.*, *58*(212), 1227–1244, doi:10.3189/2012JoG12J003.
- Horgan, H. J., and S. Anandakrishnan (2006), Static grounding lines and dynamic ice streams: Evidence from the Siple Coast, West Antarctica, *Geophys. Res. Lett.*, *33*, L18502, doi:10.1029/2006GL027091.
- Jenkins, A. (2011), Convection-driven melting near the grounding lines of ice shelves and tidewater glaciers, *J. Phys. Oceanogr.*, *41*(12), 2279–2294, doi:10.1175/JPO-D-11-03.1.
- Langley, K., A. von Deschanden, J. Kohler, A. Sinisalo, K. Matsuoka, T. Hattermann, A. Humbert, O. A. Nost, and E. Isaksson (2014), Complex network of channels beneath an Antarctic ice shelf, *Geophys. Res. Lett.*, *41*, 1209–1215, doi:10.1002/2013GL058947.
- Le Brocq, A. M., et al. (2013), Evidence from ice shelves for channelized meltwater flow beneath the Antarctic Ice Sheet, *Nat. Geosci.*, *6*(11), 945–948, doi:10.1038/NNGEO1977.
- MacAyeal, D. R. (1984), Thermohaline circulation below the Ross Ice Shelf: A consequence of tidally induced vertical mixing and basal melting, *J. Geophys. Res.*, *89*(C1), 597–606, doi:10.1029/JC089C01p00597.

- Makinson, K., P. R. Holland, A. Jenkins, K. W. Nicholls, and D. M. Holland (2011), Influence of tides on melting and freezing beneath Filchner-Ronne Ice Shelf, Antarctica, *Geophys. Res. Lett.*, *38*, L06601, doi:10.1029/2010GL046462.
- Millgate, T., P. R. Holland, A. Jenkins, and H. L. Johnson (2013), The effect of basal channels on oceanic ice-shelf melting, *J. Geophys. Res. Oceans*, *118*, 6951–6964, doi:10.1002/2013JC009402.
- Moholdt, G., L. Padman, and H. A. Fricker (2014), Basal mass budget of Ross and Filchner-Ronne ice shelves, Antarctica, derived from Lagrangian analysis of ICESat altimetry, *J. Geophys. Res. Earth Surf.*, *119*, 2361–2380, doi:10.1002/2014JF003171.
- Paolo, F. S., H. A. Fricker, and L. Padman (2015), Volume loss from Antarctic ice shelves is accelerating, *Science*, *348*(6232), 327–331, doi:10.1126/science.aaa0940.
- Rignot, E., and S. S. Jacobs (2002), Rapid bottom melting widespread near Antarctic Ice Sheet grounding lines, *Science*, *296*(5575), 2020–2023, doi:10.1126/science.1070942.
- Rignot, E., and K. Steffen (2008), Channelized bottom melting and stability of floating ice shelves, *Geophys. Res. Lett.*, *35*, L02503, doi:10.1029/2007GL031765.
- Rignot, E., S. Jacobs, J. Mouginot, and B. Scheuchl (2013), Ice-shelf melting around Antarctica, *Science*, *341*(6143), 266–270, doi:10.1126/science.1235798.
- Scambos, T., T. Haran, M. Fahnestock, T. Painter, and J. Bohlander (2007), MODIS-based Mosaic of Antarctica (MOA) Data Sets: Continent-wide surface morphology and snow grain size, *Remote Sens. Environ.*, *111*, 242–257, doi:10.1016/j.rse.2006.12.020.
- Scheuchl, B., J. Mouginot, and E. Rignot (2012), Ice velocity changes in the Ross and Ronne sectors observed using satellite radar data from 1997 and 2009, *Cryosphere*, *6*, 1019–1030, doi:10.5194/tc-6-1019-2012.
- Sergienko, O. V. (2013), Basal channels on ice shelves, *J. Geophys. Res. Earth Surf.*, *118*, 1342–1355, doi:10.1002/jgrf.20105.
- Siegfried, M. R. (2015), Investigating Antarctic ice sheet subglacial processes beneath the Whillans Ice Plain, West Antarctica, using satellite altimetry and GPS, PhD thesis, Univ. of California, San Diego, Calif.
- Siegfried, M. R., H. A. Fricker, M. Roberts, T. A. Scambos, and S. Tulaczyk (2014), A decade of West Antarctic subglacial lake interactions from combined ICESat and CryoSat-2 altimetry, *Geophys. Res. Lett.*, *41*, 891–898, doi:10.1002/2013GL058616.
- Stanton, T. P., W. J. Shaw, M. Truffer, H. F. J. Corr, L. E. Peters, K. L. Riverman, R. Bindshadler, D. M. Holland, and S. Anandakrishnan (2013), Channelized ice melting in the ocean boundary layer beneath Pine Island Glacier, Antarctica, *Science*, *341*(6151), 1236–1239, doi:10.1126/science.1239373.
- Vaughan, D. G., H. F. J. Corr, R. A. Bindshadler, P. Dutrieux, G. H. Gudmundsson, A. Jenkins, T. Newman, P. Vornberger, and D. J. Wingham (2012), Subglacial melt channels and fracture in the floating part of Pine Island Glacier, Antarctica, *J. Geophys. Res.*, *117*, F03012, doi:10.1029/2012F002360.
- Winberry, J. P., S. Anandakrishnan, R. B. Alley, D. A. Wiens, and M. J. Pratt (2014), Tidal pacing, skipped slips and the slowdown of Whillans Ice Stream, Antarctica, *J. Glaciol.*, *60*(222), 795–807, doi:10.3189/2014JoG14J038.